A study of the pointed observation methods and sensitivity of HXMT*

JIN Jing(金晶)[1,2;1)] CHEN Yong(陈勇)[3] ZHANG Shuang-Nan(张双南)[4,2,3]
ZHANG Shu(张澍)[3] LI Xin-Qiao(李新乔)[3] LI Gang(李刚)[3]

[1] Department of Engineering Physics, Tsinghua University, Beijing 100084, China
[2] Center for Astrophysics, Tsinghua University, Beijing 100084, China
[3] Key Laboratory of Particle Astrophysics, Institute of High Energy Physics, Chinese Academy of Sciences, Beijing 100049, China
[4] Department of Physics, Tsinghua University, Beijing 100084, China

Abstract The Hard X-ray Modulation Telescope (HXMT) is an X-ray astronomy satellite consisting of three slat-collimated instruments, the High Energy X-ray Instrument (HE), the Medium Energy X-ray Instrument (ME), and the Low Energy X-ray Instrument (LE). HXMT will carry out an all sky survey and make pointed observations in the 1–250 keV energy band. In order to get the source and background fluxes simultaneously in the pointed observations, two methods, i.e., the combined field of view (FOV) method and the off-axis pointing method are proposed in this paper. Comprehensive analyses of the sensitivities of the three instruments by using these two methods are presented, respectively. It is found that the off-axis pointing method has a higher sensitivity for HE and ME but a lower sensitivity for LE. Since the axes of the three instruments are aligned along the same direction, the off-axis pointing method is recommended as the main method in the pointed observation for HXMT; the combined FOV method can be used when LE is the most relevant instrument in order to satisfy the scientific objective of the observation.

Key words HXMT, pointed observation, sensitivity, off-axis

PACS 90.

1 Introduction

The Hard X-ray Modulation Telescope (HXMT) is an X-ray satellite devoted to a sensitive all-sky survey and pointed observations in 1–250 keV [1]. It has three slat-collimated instruments: the Low Energy X-ray Instrument (LE, 1–15 keV), the Medium Energy X-ray Instrument (ME, 5–30 keV) and the High Energy X-ray Instrument (HE, 20–250 keV). The axes of the three instruments are aligned with each other and their fields of view (FOVs) are comparable. In the all-sky survey, HXMT scans the whole sky, and the X-ray images are reconstructed from the scanning data by using the direct demodulation method developed by Li and Wu [2]. In the pointed observations, the source and background events cannot be distinguished from each other. Therefore, the determination of the source flux is highly correlated with the estimated background flux.

Fortunately, the background and source influence the detected count rate in different ways. The in-orbit background of a slat-collimated X-ray instrument can be divided into two categories: the Cosmic X-ray Background (CXB) incident from the FOVs and the local background induced by the interaction of the satellite with the surrounding high energy particles, called the Particle Background (PB) here. CXB is uniform, and its contribution to the detected background count rate is proportional to the size of the FOV and does not vary with time or the pointing direction. On the other hand, PB is almost unrelated to the FOV and the pointing direction but varies with time. The source count rate changes with the pointing direction of the instrument. If the source is on the instrument axis, the source count rate is the highest and this value does not change with the FOV size.

Received 18 February 2009, Revised 11 March 2009
* Supported by National Basic Research Program of China (973 Program 2009CB824800)
1) E-mail: jinj02@mails.tsinghua.edu.cn

However, the source count rate will decrease when the source offsets from the axis, since part of the detector will be shadowed by the collimator. These differences could be used to determine the source and simultaneously background fluxes.

The on-off method has traditionally been used as the method to get the source flux. The instrument is first pointed to the source and the recorded count rate is the sum of the source and the background. Then the instrument is pointed away from the source and records only the background count rate. The source flux can be obtained by subtracting the second count rate from the first. However, this method cannot take the temporal variability of PB into account. Thus the source flux obtained is unreliable. In order to measure the source and background fluxes simultaneously, the High Energy X-ray Timing Experiment (HEXTE) on board the Rossi X-ray Timing Explorer (RXTE) used an improved on-off method: one cluster was pointed to the source and the other was offset, looking at blank sky to record the background counts; the two clusters changed the pointing directions regularly to eliminate the effect of systematic errors [3]. For HXMT, since the axes of all the instrument modules are aligned along the same direction, the method used by RXTE/HEXTE is not applicable.

To determine the source and the background fluxes simultaneously, we propose in this paper two methods for HXMT in pointed observations based on its own characteristics: the combined FOV method and the off-axis pointing method. We compare the sensitivities of the two methods and recommend the latter method as the main method that will be used by HXMT.

2 The flux determination methods and the sensitivity calculation principles

2.1 The combined FOV method

For the combined FOV method, the targeted source is located right on the axis of the instruments; each instrument has several different FOVs so as to measure the contribution of different background contributions. HE is taken as an example to illustrate the combined FOV method and the principles of sensitivity calculation. The situation for ME and LE is similar.

HE has eighteen identical detecting modules. Each module is equipped with a collimator in front of it to form the FOV. There are three types of collimators according to their FOV sizes: the small FOV collimator, the large FOV collimator and the covered FOV collimator. The number of small FOV modules is much larger than the number of the other two kinds of modules and the size of the small FOV is recommended to be $6^\circ \times 1^\circ$. This selection is made for reasons below. Firstly, if the FOV size is too big, CXB entering from the FOV of the collimator will be very high, which will greatly increase the noise-to-signal ratio in the pointed observation. If the FOV size is too small, the source photons incident from the FOV will be very few in the scan survey, leading to a low survey sensitivity. In addition, in this situation, decreasing the FOVs helps little in the background reduction for the pointed observation, since the FOV independent PB becomes dominant. A good balance between the capability of the pointed observation and the scan survey will be reached when CXB and PB are approximately the same. Simulations show that, when the FOV size is $6^\circ \times 1^\circ$, PB is higher than CXB for HE and lower for LE; for ME, the two are about the same. Therefore HXMT reaches the best overall capability with this FOV. Furthermore, for the imaging observation, increasing the FOV size can improve the sensitivity but may worsen the resolution of the image. A FOV of $6^\circ \times 1^\circ$ can also meet both the sensitivity and resolution demands[1)]. Besides the dominant small FOV modules, there are several large-sized FOV modules which are used for the measurement of CXB and some covered FOV modules to measure PB directly.

As discussed in the last section, the count rate in each module caused by CXB is proportional to the size of the FOV and the PB contribution is the same for different modules, even if it is covered. Since the target source is located right on the axis, the source count rate is expected to be the same for all the modules that are not covered. Based on these analyses, the following three equations hold:

$$C_{\rm s} = n \times T \times (f_{\rm s} \times A + f_{\rm cx} \times V_{\rm s} + f_{\rm p}), \quad (1)$$

$$C_{\rm l} = m \times T \times (f_{\rm s} \times A + f_{\rm cx} \times V_{\rm l} + f_{\rm p}), \quad (2)$$

$$C_{\rm c} = k \times T \times f_{\rm p}, \quad (3)$$

where $C_{\rm s}$ denotes the total counts in all the small FOV modules; $C_{\rm l}$ and $C_{\rm c}$ denote the total counts in all the large FOV modules and the covered FOV modules respectively. n, m and k denote the numbers of

1) Shen Zong-Jun. Studies and Applications of Direct Demodulate Method. Tsinghua University, doctoral dissertation, 2007 (in Chinese)

small FOV, large FOV and covered FOV modules respectively. T is the observation time, which is taken as 1000 seconds through out this paper. $f_{\rm s}$ is the flux of the source, in units of cts$\cdot$s$^{-1}\cdot$cm^{-2}, and A is the effective area of each module taking the detection efficiency into account. $f_{\rm cx}$ is the count rate caused by CXB in one square degree FOV for each module, in units of cts$\cdot$s$^{-1}\cdot$deg^{-2}; $f_{\rm p}$ is the count rate caused by PB in each module. $V_{\rm s}$ and $V_{\rm l}$ represent the size of small FOV and large FOV respectively, in units of square degree. By solving the above equations, $f_{\rm s}$ can be obtained as follows,

$$f_{\rm s}=\frac{1}{A\times T}\times\left[\frac{C_{\rm s}\times V_{\rm l}}{n\times(V_{\rm l}-V_{\rm s})}-\frac{C_{\rm c}}{k}-\frac{C_{\rm l}\times V_{\rm s}}{m\times(V_{\rm l}-V_{\rm s})}\right]. \quad (4)$$

The error of $f_{\rm s}$ is given by,

$$\sigma_{f_{\rm s}}=\frac{1}{A\times T}\left[\frac{V_{\rm l}^2\times C_{\rm s}}{n^2\times(V_{\rm l}-V_{\rm s})^2}+\frac{C_{\rm c}}{k^2}+\frac{V_{\rm s}^2\times C_{\rm l}}{m^2\times(V_{\rm l}-V_{\rm s})^2}\right]^{\frac{1}{2}}. \quad (5)$$

Thus, $\sigma_{f_{\rm s}}/f_{\rm s}$ is the noise-to-signal ratio of the source flux. The value of $f_{\rm s}$ which makes $f_{\rm s}/\sigma_{f_{\rm s}}=5$ is defined as the sensitivity at 5σ, whose statistical meaning can be found from Zhang & Ramsden (1990) [4].

2.2 The off-axis method

For the off-axis observation method, all the modules for an instrument are divided on average into three groups according to the major axis directions of the FOVs. The angles between different major axes are all 60 degrees, as shown in Fig. 1. The coordinate system used to describe the off-axis position is also plotted in Fig. 1. In fact, the best pointed observation sensitivity is achieved when all the modules for each instrument are divided on average into two groups with a 90° angle between different major axes. However, the three group scheme is chosen for several reasons. Firstly, both ME and LE are designed to have three detectors, after considering many factors, which cannot easily be divided into two groups on average, as shown in Fig. 2. Secondly, the three group scheme gives a better imaging quality in the all-sky survey. Thirdly, the pointed observation sensitivity difference of the two schemes is marginal. With all things considered, the three group scheme is recommended[1)].

If the source is located in the center of the FOV, namely, on the axis of the instrument, the source count rate for each module is the same. However, if the instrument is pointed away from the source by a small angle, the source count rates will be dissimilar for modules in different groups, since their projected area is not the same. Nevertheless, the background count rates in all the detecting modules are the same no matter which groups they are in. Therefore, it is possible to obtain the source and background fluxes simultaneously by pointing the instrument away from the source by a small angle.

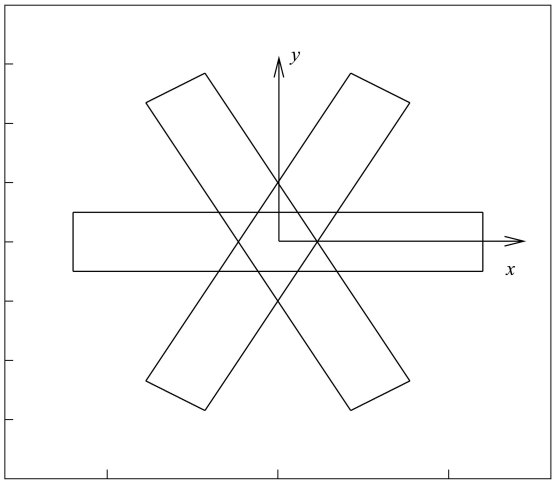

Fig. 1. A sketch of the FOV directions of three groups.

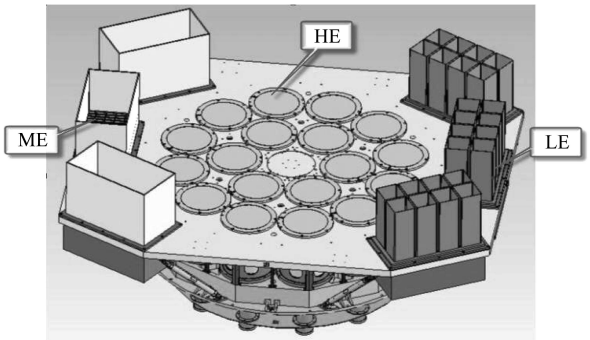

Fig. 2. A sketch of HXMT's mechanical structure.

It should be mentioned that in the off-axis observation, there are also small FOV modules, large FOV modules and covered modules, and they are the same as those in the combined FOV method discussed in Section 2.1. However, the last two kinds of modules do not help much in the improvement of the off-axis observation sensitivity. They are used for other goals such as to measure the CXB and PB contributions.

Based on the above principles, six equations can be obtained for the off-axis method:

$$C_{1{\rm s}} = n\times T\times(f_{\rm s}\times A\times a_{1{\rm s}}+f_{\rm cx}\times V_{\rm s}+f_{\rm p}), \quad (6)$$

$$C_{1{\rm l}} = m\times T\times(f_{\rm s}\times A\times a_{1{\rm l}}+f_{\rm cx}\times V_{\rm l}+f_{\rm p}), \quad (7)$$

1) Shen Zong-Jun. Studies and Applications of Direct Demodulate Method. Tsinghua University, doctoral dissertation, 2007 (in Chinese)

$$C_{2s} = n\times T\times(f_s\times A\times a_{2s}+f_{cx}\times V_s+f_p), \quad (8)$$

$$C_{2l} = m\times T\times(f_s\times A\times a_{2l}+f_{cx}\times V_l+f_p), \quad (9)$$

$$C_{3s} = n\times T\times(f_s\times A\times a_{3s}+f_{cx}\times V_s+f_p), \quad (10)$$

$$C_{3l} = m\times T\times(f_s\times A\times a_{3l}+f_{cx}\times V_l+f_p), \quad (11)$$

where C_{1s} denotes the total counts in the small FOV modules of group one. The subscripts s and l denote the large FOV and small FOV respectively; the subscript number denotes group number. Thus, C_{2s} and C_{3s} have similar meanings to C_{1s} but for groups two and three respectively. n and m are the numbers of the small FOV modules and the large FOV modules in each group. T, f_s, A, f_{cx}, f_p, V_s and V_l have the same meaning as those in Eqs. (1), (2) and (3) in Section 2.1. a is the fraction of the projected area.

The source flux (f_s) can be obtained from different combinations of the above equations. We try several combinations and find that the combination $C_{1s}-(C_{2s}+C_{3s})/2$ can give the smallest noise-to-signal ratio when small FOV modules dominate; the combinations $C_{3s}-(C_{1s}+C_{2s})/2$ and $C_{2s}-(C_{1s}+C_{3s})/2$ give the same noise-to-signal ratio since Eq. (6), Eqs. (8) and Eq. (10) are on an equal footing. Therefore we have

$$f_s = \frac{C_{1s}-\dfrac{C_{2s}+C_{3s}}{2}}{n\times T\times A\times\left(a_{1s}-\dfrac{a_{2s}+a_{3s}}{2}\right)}, \quad (12)$$

and

$$\sigma_{f_s} = \frac{\sqrt{C_{1s}+\dfrac{1}{4}(C_{2s}+C_{3s})}}{n\times T\times A\times\left(a_{1s}-\dfrac{a_{2s}+a_{3s}}{2}\right)}. \quad (13)$$

The value of f_s that makes $f_s/\sigma_{f_s}=5$ is the sensitivity at 5 σ.

In our calculation, a region of x from -3° to 3°, y from -3° to 3° is searched, which is large enough to include the best off-axis position. The step length is 0.01° for both x and y, The sensitivity at each position in this region is calculated to find the one which gives the best sensitivity.

3 Calculations and results

The background data used in this paper come from the simulation results by Li Gang et al[1)]. The detection efficiency and the geometrical area of the detectors used to calculate the effective area are given by Li Xin-Qiao[2)].

3.1 HE

HE has eighteen modules, including fifteen with the small FOV ($6^\circ\times 1^\circ$), two with the large FOV ($6^\circ\times 6^\circ$), and one with the FOV covered.

The count rate caused by CXB in a one square degree FOV for all the modules of each instrument is called B_{c0} and the count rate caused by PB for all the modules of each instrument is called B_p here. B_{c0} is equal to f_{cx} in Eq. (1) multiplied by the number of modules of each instrument and B_p is equal to f_p in Eq. (1) multiplied by that number. For HE, B_{c0} is 2.77 cts$\cdot$s$^{-1}\cdot$deg^{-2} and B_p is 183.4 cts$\cdot$s^{-1}. The effective area calculated for HE is 3611 cm^2.

In the off-axis mode, a region of x from -3° to 3°, y from -3° to 3° is searched to find the best off-axis angle, as mentioned in the last paragraph of Section 2.2. The best off-axis angle calculated is $(x,y)=(1.16^\circ,0^\circ)$ and the sensitivity at this off-axis angle is regarded as the sensitivity given by the off-axis method. At this off-axis angle, two groups of modules only record the background photons and the other group of modules has the largest projected area for the source.

Since the actual in-orbit PB may be different from the simulated value by one order of magnitude, sensitivities with different PB values, ranging from a quarter of to four times the current simulation B_p, are calculated in both the combined FOV method and the off-axis method. The 5 σ sensitivity results are listed in Table 1 and plotted in Fig. 3.

For HE, the sensitivity given by the off-axis method is better than that given by the combined FOV method. This is mainly because the combined FOV method uses the covered FOV modules to estimate PB. When the PB value is big and the number

Table 1. 5 σ sensitivities given by the combined FOV method and the off-axis method for HE with different PB values. A one mCrab source causes a total count rate of 0.7 cts$\cdot$s^{-1} for HE.

	0.25 B_p	0.5 B_p	1 B_p	2 B_p	4 B_p
combined FOV method	7.4 mCrab	10 mCrab	14 mCrab	20 mCrab	29 mCrab
off-axis method	5.4 mCrab	7.1 mCrab	9.6 mCrab	13 mCrab	19 mCrab

1) Li Gang, Li Xin-Qiao, Zhang Shu. The HXMT document (HXMTK-002) (in Chinese)

2) Li Xin-Qiao. The HXMT document (HXMTK-003) (in Chinese)

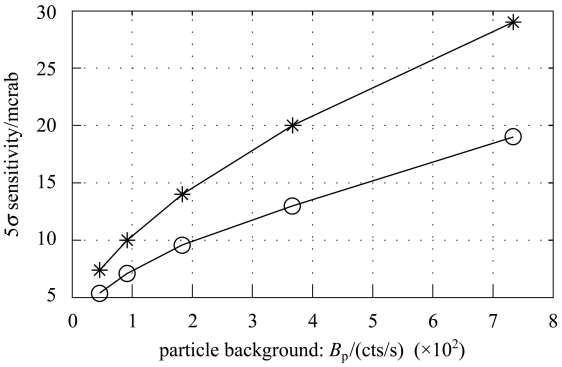

Fig. 3. 5 σ sensitivities given by the combined FOV method and the off-axis method for HE with different PB values. The line with * denotes the sensitivity of the combined FOV method, and the line with circles denotes the sensitivity of the off-axis method.

of covered FOV modules is small, the error of PB is very big (C_c/k^2 in formula (5)), which contributes a big error to the deduced source flux. This big error can be reduced by increasing the number of covered FOV modules. However, this proposal has not been adopted since it will greatly reduce the effective area of the instrument. For the off-axis method, two groups of modules are used to measure the total background, which makes the measurement more accurate. This is why the off-axis method gives a better sensitivity. In the case of LE below, the PB value is very small, so the combined FOV method gives a better sensitivity than the off-axis method.

3.2 ME

ME has 54 modules in total, including 45 small FOV modules, six large FOV ($6^\circ \times 6^\circ$) modules and three covered ones. The size of the small FOV has two options: $1^\circ \times 1^\circ$ or $6^\circ \times 1^\circ$ the ($1^\circ \times 1^\circ$ choice is provided only for the consideration that it may improve the sensitivity of the combined FOV method).

For ME, B_{c0} is 1.49 cts$\cdot$s$^{-1}\cdot$deg^{-2} and B_p is 28 cts$\cdot$s^{-1}. The calculated effective area for ME is 690 cm^2.

The calculated sensitivity of the combined FOV method and the off-axis method are listed in Table 2 and plotted in Fig. 4. The sensitivity results for the small FOV size of $1^\circ \times 1^\circ$ and $6^\circ \times 1^\circ$ are also given for comparison.

Table 2. 5 σ sensitivities given by the combined FOV method and the off-axis method for ME with different PB values. A one mCrab source causes a total count rate of 0.6 cts$\cdot$s^{-1} for ME.

	0.25 B_p	0.5 B_p	1 B_p	2 B_p	4 B_p
combined FOV $1^\circ \times 1^\circ$	3.2 mCrab	4.5 mCrab	6.4 mCrab	9.0 mCrab	12.8 mCrab
combined FOV $6^\circ \times 1^\circ$	3.7 mCrab	4.9 mCrab	6.7 mCrab	9.4 mCrab	13.1 mCrab
off-axis $1^\circ \times 1^\circ$	28.2 mCrab	36.5 mCrab	49.9 mCrab	69.2 mCrab	96.8 mCrab
off-axis $6^\circ \times 1^\circ$	3.2 mCrab	3.9 mCrab	4.9 mCrab	6.4 mCrab	8.8 mCrab

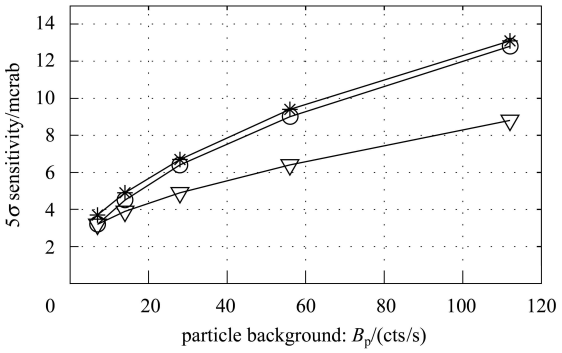

Fig. 4. 5 σ sensitivities given by the combined FOV method and the off-axis method for ME with different PB values. The line with * denotes the sensitivity of the combined FOV method when the small FOV is $6^\circ \times 1^\circ$; the line with circles denotes the sensitivity of the combined FOV method when the small FOV is $1^\circ \times 1^\circ$; the line with ∇ denotes the sensitivity of the off-axis method when the small FOV is $6^\circ \times 1^\circ$.

If the size of the small FOV is $1^\circ \times 1^\circ$, the sensitivity given by the off-axis method is very bad. This is because for the $1^\circ \times 1^\circ$ FOV, the best sensitivity is reached at the off-axis position $(x, y) = (1.00^\circ, 0^\circ)$ instead of the natural best off-axis position $(x, y) = (1.16^\circ, 0^\circ)$ due to the limitation of the FOV size. Thus, a FOV of $1^\circ \times 1^\circ$ is not suitable for the off-axis method.

For ME, the sensitivity given by the off-axis method with the small FOV size of $6^\circ \times 1^\circ$ is the best of all. The best sensitivity is also reached at the position $(x, y) = (1.16^\circ, 0^\circ)$ in the off-axis method.

3.3 LE

LE has 96 modules in total, including 68 with the small FOV, 22 with the large FOV ($6^\circ \times 6^\circ$) and six with the FOV covered. Like ME, the size of the small FOV has two options: $1^\circ \times 1^\circ$ or $6^\circ \times 1^\circ$. LE's energy band is 1–15 keV; however, the 1–6 keV band has the

best sensitivity because of the low PB; therefore only the sensitivity in the 1–6 keV energy band is calculated to evaluate the different methods. For LE, B_{c0} is 1.28 cts$\cdot$s$^{-1}\cdot$deg^{-2} and B_p is 0.71 cts$\cdot$s^{-1} for 1-6 keV. The effective area calculated for LE is 282 cm^2.

The calculated sensitivity values of the combined FOV method and the off-axis method are listed in Table 3 and plotted in Fig. 5. Similar to ME, if the size of the small FOV is $1^\circ\times1^\circ$, the sensitivity of the off-axis method is very bad, and thus this case is not considered for LE.

Table 3. 5 σ sensitivities given by the combined FOV method and the off-axis method for LE with different PB values. A one mCrab source causes a total count rate of 1.5 cts$\cdot$s^{-1} for LE.

	0.25 B_p	0.5 B_p	1 B_p	2 B_p	4 B_p	8 B_p	10 B_p
combined FOV $1^\circ\times1^\circ$	0.26 mCrab	0.32 mCrab	0.42 mCrab	0.57 mCrab	0.78 mCrab	1.09 mCrab	1.21 mCrab
combined FOV $6^\circ\times1^\circ$	0.57 mCrab	0.61 mCrab	0.67 mCrab	0.77 mCrab	0.95 mCrab	1.22 mCrab	1.34 mCrab
off-axis $6^\circ\times1^\circ$	0.98 mCrab	0.99 mCrab	1.01 mCrab	1.05 mCrab	1.13 mCrab	1.26 mCrab	1.33 mCrab

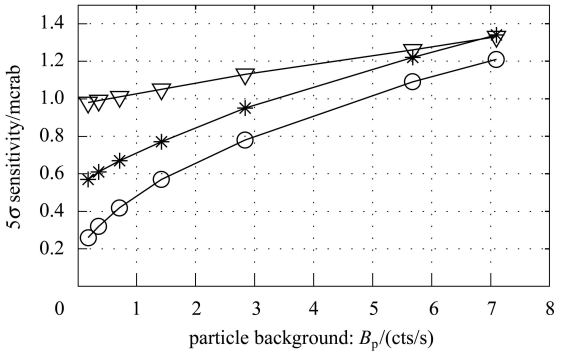

Fig. 5. 5 σ sensitivities given by the combined FOV method and the off-axis method for LE with different PB values. The line with circles denotes the sensitivity values of the combined FOV method when the small FOV is $1^\circ\times1^\circ$; the line with * denotes the sensitivity values of the combined FOV method when the small FOV is $6^\circ\times1^\circ$; the line with ∇ denotes the sensitivity values of the off-axis method when the small FOV is $6^\circ\times1^\circ$.

For LE, the sensitivity given by the combined FOV method with $1^\circ\times1^\circ$ FOV is the best, mainly due to the very low PB. However, the axes of HE, ME and LE are aligned along the same direction and the off-axis method with small FOV $6^\circ\times1^\circ$ gives the best sensitivity for both HE and ME. Thus, the off-axis method with the small FOV of $6^\circ\times1^\circ$ is also recommended for LE. The combined FOV method can be used when LE is the most relevant instrument in order to satisfy the scientific objective of the observation.

4 Summary

In order to get the best sensitivity in the pointed observation for HXMT, sensitivities given by the combined FOV method and the off-axis method have been calculated and compared. It has been shown that for HE and ME, the off-axis method gives a better sensitivity than the combined FOV method and the best off-axis position is $(x,y)=(1.16^\circ,0^\circ)$. For LE, the combined FOV method gives a better sensitivity. Since the axes of the three instruments are aligned along the same direction, the off-axis pointing method is recommended as the main method in the pointed observation for HXMT; the combined FOV method can be used when LE is the most relevant instrument in order to satisfy the scientific objective of the observation. The correspondingly recommended FOV combinations for the three instruments are listed in Table 4.

Table 4. The recommended FOV combinations for HE, ME and LE.

	$6^\circ\times1^\circ$ FOV	$6^\circ\times6^\circ$ FOV	covered
HE	15	2	1
ME	45	6	3
LE	68	22	6

References

1 LI Ti-Pei, ZHANG Shuang-Nan, LU Fang-Jun. Chin. J. Space Sci, 2006, **26(Supp)**: 30–41
2 LI Ti-Pei, WU Mei. Ap & SS, 1994, **215**: 213
3 Rothschild R E, Blanco P R, Gruber D E et al. The Astrophysical Journal, 1998, **496**: 538–549
4 ZHANG Shuang-Nan, Ramsden D. Experimental Astronomy, 1990, **1**: 145–163